29th International Cosmic Ray Conference Pune (2005) **3**, 13–16

Measurement of cosmic-ray antiproton spectrum with BESS-2002

S. Haino[a], K. Abe[b*], H. Fuke[c], T. Maeno[b†], Y. Makida[a], S. Matsuda[d], H. Matsumoto[d], J.W. Mitchell[e], A.A. Moiseev[e], J. Nishimura[d], M. Nozaki[b], S. Orito[d‡], J.F. Ormes[e], T. Sanuki[d], M. Sasaki[e], E.S. Seo[f], Y. Shikaze[b§], R.E. Streitmatter[e], J. Suzuki[a], K. Tanaka[a], T. Yamagami[c], A. Yamamoto[a], T. Yoshida[a] and K. Yoshimura[a]

(a) High Energy Accelerator Research Organization (KEK), Tsukuba, Ibaraki 305-0801 Japan
(b) Kobe University, Kobe, Hyogo 657-8501 Japan
(c) The Institute of Space and Astronautical Science (ISAS/JAXA), Sagamihara, Kanagawa 229-8510 Japan
(d) The University of Tokyo, Bunkyo, Tokyo 113-0033 Japan
(e) NASA Goddard Space Flight Center (NASA/GSFC), Greenbelt, MD 20771 USA
(f) University of Maryland, College Park, MD 20742 USA
Presenter: S. Haino (haino@post.kek.jp), jap-haino-S-abs1-og11-oral

We report a cosmic-ray antiproton spectrum measured with the BESS balloon experiment performed in 2002, which was in an intermediate period between the solar maximum in 2000 and the coming solar minimum. The observed antiproton spectrum and the antiproton to proton ratio are crucial for further development of the drift model of the solar modulation effect which has been generally supported by the previous measurements.

1. Introduction

The energy spectrum of cosmic-ray antiprotons has been successively measured at Lynn Lake, Canada by BESS experiments since 1993 [1, 2, 3]. It revealed that the cosmic-ray antiproton spectrum has a distinct peak around 2 GeV, indicating a characteristic feature of secondary antiprotons produced by cosmic-ray interactions with interstellar gas. However, we still have some possibilities of exotic primary origins [4]. As well as measurements of the cosmic-ray antiproton spectrum with much higher accuracy, the detailed understanding of the secondary antiproton spectrum including the solar modulation effect is important to discuss about the existence of the primary origins. During the positive polarity phase of the solar activity until 1999 the measured antiproton to proton ($\bar{p}/p$) ratio [2] showed no distinctive variation. After the reversal at the solar magnetic field in 2000, a sudden increase of the $\bar{p}/p$ ratio [3] was clearly observed. Our measurements, as well as other measurements [5], generally support the recent calculations [6, 7] incorporating the steady-state drift model and charge-dependent effects of the solar modulation. Protons and antiprotons have sharply different interstellar spectra and the drift directions are opposite due to the opposite charge sign. The combination of these effects implies that the $\bar{p}/p$ ratio should display a more interesting evolution [6] during 2000-2010 than it did during the 1990's. We report here a new measurement of cosmic-ray antiproton spectrum performed in 2002, which was an intermediate period between the last solar maximum and the next solar minimum.

2. Spectrometer

The BESS spectrometer [8] has been upgraded several times [9] since the first flight in 1993. In 2002, a new tracking system was developed to achieve better momentum resolution and the spectrometer was upgraded as

* Present address: Kamioka observatory, ICRR, The University of Tokyo, Kamioka-cho, Gifu 506-1205 Japan
† Present address: Brookhaven National Laboratory, Upton, NY 11973-5000 USA
‡ Deceased
§ Present address: Tokai Research Establishment, Japan Atomic Energy Research Institute, Tokai, Ibaraki 391-1195 Japan

the BESS-TeV spectrometer [10]. As shown in Figure 1, the spectrometer has a unique feature of a cylindrical configuration realized by a thin superconducting solenoid. In the central region, the solenoid with a diameter of 1 m provides a uniform magnetic field of 1 T. A magnetic-rigidity ($R \equiv pc/Ze$) of the incoming particle is determined from a deflection (R^{-1}) of the trajectory measured by a tracking system consisting a central jet-type drift chamber (JET), two inner drift chambers (IDCs) and two outer drift chambers (ODCs). Inside the JET and IDCs the deflection was obtained by a circular fitting using up to 52 hit points measured with a spacial resolution less than 150 μm. The maximum detectable rigidity (MDR) of 300 GV was achieved. In the analysis of antiproton spectrum hit points inside ODCs were not used. The rigidity resolution was less than 2 % at 5 GV without ODCs and the spillover of protons can be totally rejected. Time-of-flight (TOF) counters provide the velocity (β) and energy loss (dE/dx) measurements. The albedo protons can be totally rejected with the β^{-1} resolution of 1.4 %. The spectrometer also incorporates a threshold-type Cherenkov counter with a silica-aerogel radiator which can identify antiprotons from electron and muon backgrounds up to a kinetic energy of 4 GeV. The data acquisition sequence is initiated by a first-level TOF trigger which is a simple coincidence of signals from the top and bottom TOF counters. The second-level trigger is then generated by using the hit patterns of the TOF counters and IDCs and selects negative-charged particles predominantly. In addition, one of every 10 first-level triggered events are recorded to build a unbiased samples.

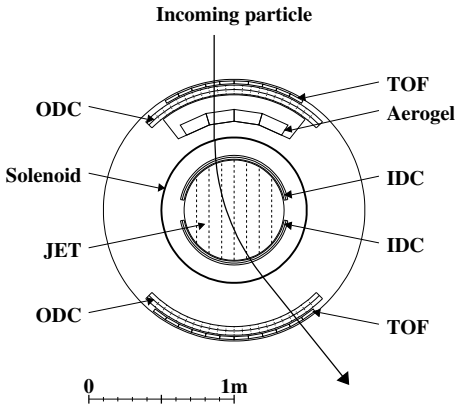

Figure 1. Cross-sectional view of the BESS spectrometer.

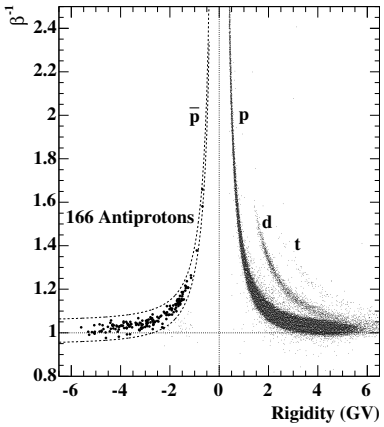

Figure 2. The mass identification plot of antiproton events. The dashed curves define the antiproton bands.

3. Observation and Analysis

The observation was carried out on 7th August 2002 in northern Canada, Lynn Lake to Ft. McMurray where the geomagnetic cutoff rigidity was 0.5 GV or smaller. The total live time of the data-taking was 38,215 seconds (10.6 hours) during the floating period at an altitude of 37 km (residual atmosphere of 4.8 g/cm^2). Among them 90 % of data with the stable enviromental condition were used to obtain the antiproton spectrum. The off-line analysis was made in the same way as our previous measurements [2, 3]. We selected events with a single track fully contained in the fiducial region of the tracking volume. The dE/dx measurements of top and bottom TOF counters and JET are loosely required as a function of rigidity to be consistent with antiprotons. These simple and highly-efficient selections are sufficient for a very clean detection of antiprotons in the low velocity ($\beta < 1/1.1$) region. At higher velocities, where electrons and muons begin to contaminate the antiproton band,

we required the Cherenkov veto, which rejected electron and muon backgrounds by a factor of 1500 while keeping 95 % efficiency for antiprotons below the threshold rigidity of 4.7 GV. Figure 2 shows the β^{-1} versus rigidity (R) plot for surviving events. 166 antiproton candidates were clearly identified. The antiproton bands are slightly contaminated by backgrounds due to the inefficiency of the Cherenkov counter. We estimated the fraction of such backgrounds to be 0 %, 0.6 % and 0.5 % at 0.3, 2 and 4 GeV, respectively. Other backgrounds such as albedo and spillover of protons were found to be negligible. The survival probabilities for antiprotons to traverse residual air and the instrument without interactions were estimated by a Monte Carlo (MC) simulation to be 62 %, 71 % and 71 % at 0.3, 2 and 4 GeV, respectively. The MC code was tuned and verified by comparing the simulation with an accelerator beam test of the spectrometer [11], and the systematic uncertainty of the survival probabilities were reduced down to 5 %. The backgrounds from atmospheric secondary antiprotons were estimated by calculations in the same way as [3]. The estimated backgrounds amounted to 27±9 %, 26±2 % and 24±8 % at 0.3, 2 and 4 GeV, respectively, where the errors correspond to the maximum difference among the results of calculations based on different models.

4. Results and Conclusion

Table 1 gives the resultant antiproton flux and $\bar{\mathrm{p}}$/p ratio at the top of the atmosphere, and Figure 3 shows the antiproton flux and $\bar{\mathrm{p}}$/p ratio together with the previous measurements [3] around the solar field reversal. The error bars represent quadratic sums of the statistical and systematic errors, and curves represent calculations of a steady-state drift model [6, 7] in which the modulation is characterized by a tilt angle of the heliospheric current sheet and the Sun's magnetic polarity. Periods at $70°(+)$, $70°(-)$ and $40°(-)$ roughly correspond to the years of 1999, 2000 and 2002, respectively [12]. For the antiproton spectrum, the results of the calculations do not fully reproduce the overall features of the spectrum modulation. For the $\bar{\mathrm{p}}$/p ratio, however, the results of the calculation is consistent with the data within the errors. The $\bar{\mathrm{p}}$/p ratio cancels the solar modulation effect common to charged particles, and emphasizes the effect of charge-sign dependence. The observed data are the crucial for further development of the model with more realistic parameters and the time dependence.

The accurate calculation of the secondary antiproton spectrum including the solar modulation effect is inevitably important. It can estimate a "background" in searching for antiprotons from exotic primary origins [4] by new measurements with much higher statistics, such as BESS-Polar [13] long duration balloon (LDB) flight over Antarctica, and forthcoming space-based experiments such as PAMELA and AMS.

Table 1. Antiproton flux and $\bar{\mathrm{p}}$/p ratio at the top of atmosphere with the statistical (first) and systematic (second) errors. $N_{\bar{\mathrm{p}}}$ is the number of observed antiprotons.

Kinetic energy (GeV) range	mean	$N_{\bar{\mathrm{p}}}$	$\bar{\mathrm{p}}$ flux ($\mathrm{m^{-2}sr^{-1}s^{-1}GeV^{-1}}$)	$\bar{\mathrm{p}}$/p ratio
0.18–0.56	0.32	3	$2.10\,^{+1.32+0.28}_{-1.61-0.28}\times10^{-3}$	$6.95\,^{+4.38+1.13}_{-5.33-1.13}\times10^{-6}$
0.56–0.78	0.69	9	$8.82\,^{+2.61+1.25}_{-3.72-1.25}\times10^{-3}$	$2.48\,^{+0.73+0.38}_{-1.04-0.38}\times10^{-5}$
0.78–1.10	0.96	22	$1.84\,^{+0.39+0.13}_{-0.44-0.13}\times10^{-2}$	$5.50\,^{+1.17+0.47}_{-1.33-0.47}\times10^{-5}$
1.10–1.53	1.30	18	$1.08\,^{+0.25+0.16}_{-0.29-0.16}\times10^{-2}$	$3.57\,^{+0.83+0.56}_{-0.95-0.56}\times10^{-5}$
1.53–2.15	1.89	29	$1.66\,^{+0.30+0.21}_{-0.33-0.21}\times10^{-2}$	$6.64\,^{+1.18+0.86}_{-1.33-0.86}\times10^{-5}$
2.15–3.00	2.58	34	$1.41\,^{+0.24+0.15}_{-0.26-0.15}\times10^{-2}$	$7.78\,^{+1.30+0.90}_{-1.45-0.90}\times10^{-5}$
3.00–4.20	3.50	32	$1.27\,^{+0.23+0.14}_{-0.25-0.14}\times10^{-2}$	$1.01\,^{+0.18+0.12}_{-0.20-0.12}\times10^{-4}$

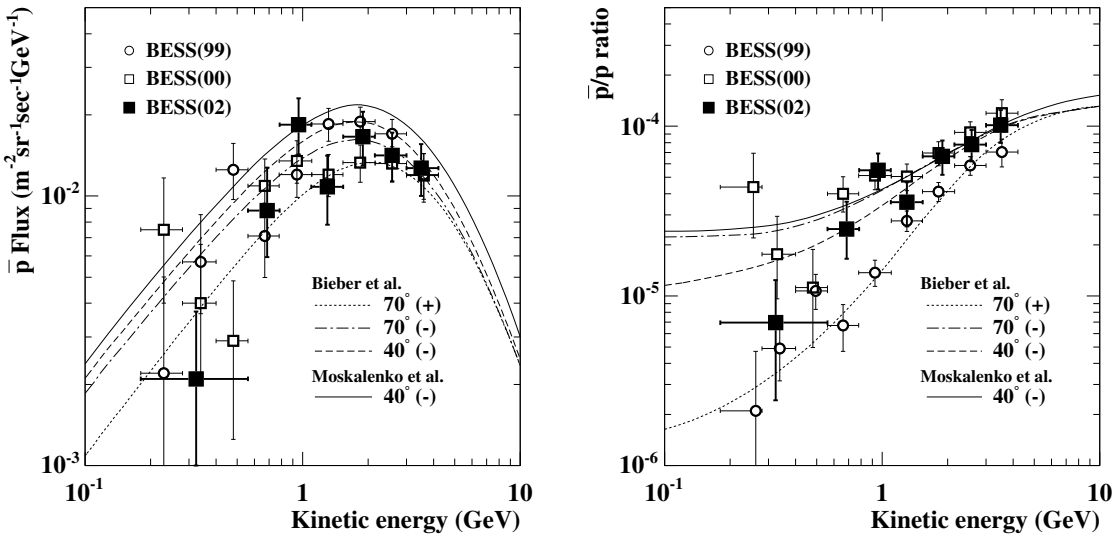

Figure 3. Antiproton flux (left) and $\bar{p}/p$ ratio (right) at the top of atmosphere together with the previous measurements [3] in 1999 and 2000. The curves represent calculations of a steady-state drift model [6, 7] at each tilt angle of the heliospheric current sheet and the Sun's magnetic polarity. Periods at $70^\circ(+)$, $70^\circ(-)$ and $40^\circ(-)$ roughly correspond to the years of 1999, 2000 and 2002.

5. Acknowledgements

This experiment is supported by Grant-in-Aid for Scientific Research on Priority Areas (12047227 and 12047206) from MEXT in Japan and by NASA in the US. We would thank ISAS, ICEPP, and KEK for their continuous support.

References

[1] S. Orito et al., Phys. Rev. Lett. 84, 1078 (2000).
[2] T. Maeno et al., Astropart. Phys. 16, 121 (2001).
[3] Y. Asaoka et al., Phys. Rev. Lett. 88, 051101 (2002).
[4] T. Mitsui et al., Phys. Lett. B 389, 160 (1996).
L. Bergström et al., Astrophs. J. 526, 215 (1999).
[5] J. Clem and P. Evenson, J. Geophys. Res. 109, A07107 (2004).
[6] J.W. Biever et al., Phys. Rev. Lett. 83, 674 (1999).
[7] I.V. Moskalenko et al., Astrophs. J. 565, 280 (2002).
[8] Y. Ajima et al., Nucl. Instr. & Meth. A 443, 71 (2000).
[9] S. Haino et al., Nucl. Instr. & Meth. A 518, 167 (2004).
[10] S. Haino et al., Phys. Lett. B 594, 35 (2004).
[11] Y. Asaoka et al., Nucl. Instr. & Meth. A 489, 170 (2002).
[12] The Wilcox Solar Observatory: http://sun.stanford.edu/~wso/
[13] T. Yoshida et al., 29th ICRC, Pune (2005) OG 1.1.
S. Matsuda et al., 29th ICRC, Pune (2005) OG 1.1.